CHAPTER 2

To determine the site of ROS generation by analyzing the formation of respiratory complexes

2.1. Introduction

2.1.1. Oxidative stress in neurodegenerative diseases

Neurodegenerative diseases are characterized by progressive loss of neurons. Overproduction of reactive oxygen species (ROS) have been implicated in disease development. ROS are chemically reactive molecules that have been shown to play a major role in the pathogenesis of neurodegenerative diseases. ROS include hydroxyl radical (·OH), free radicals (superoxide, O_2^-) and non-radicals (hydrogen peroxide, H_2O_2) (Bolisetty and Jaimes, 2013; Gandhi et al., n.d.; Halliwell, 2006). ROS are naturally produced within the biological system, playing major roles to mediate cellular activities like cell survival, inflammation and stressor responses as well as numerous diseases including muscle dysfunction, cardiovascular disorders, cancers and allergy (He and Zuo, 2015; Zuo et al., 2015, 2014). Increased ROS levels can lead to oxidative stress (OS) or cell death because of their reactivity, which is explained as the disturbance of balance between pro-oxidant and antioxidant levels (Zuo et al., 2015). The complex pathogeneses of the neurodegenerative diseases are not yet known; however, recent evidence suggests that ROS might be the culprit as increased OS has been observed in the brain of patients with neurodegenerative disorders (Albers and Flint Beal, 2000; Dias et al., 2013).

To determine the role of ROS in neurodegenerative progression, several studies have been performed in PD and AD patients (Hensley et al., 2006; Rego and Oliveira, 2003; St-Pierre et al., 2006). Although ROS might not be responsible for triggering neurodegenerative disorders, they seem to exacerbate the progression of the disease by inducing oxidative damage in the mitochondria and subsequently to the cells (Dias et al., 2013). Moreover, neuronal cells are most vulnerable to oxidative damage due to their high oxygen consumption, weak antioxidant defences and high polyunsaturated fatty acid content in the membranes (Rego and Oliveira, 2003). The accumulation of misfolded proteins appears with the pathogenesis of several neurodegenerative disorders such as PD and AD. The accumulation of these modified proteins is responsible for triggering inflammatory response in the brain, which in turn induces marked ROS generation and subsequent OS (Wyss-Coray et al., n.d.; Zuo et al., 2015). Aberrant ROS production accompanied by mitochondrial dysfunction, is linked tightly with neurodegenerative disorders (Albers and Flint Beal, 2000; Campuzano et al., n.d.; Lin and Beal, 2006; Wallace, 1999). For example, in

Huntington's disease (HD), mutant huntingtin (mHTT) interact directly with mitochondria, resulting in compromised energy supply and heightened ROS levels (Ross and Tabrizi, 2011).

Since OS seems to play a pivotal role in neurodegenerative diseases, the manipulation of ROS levels may represent an effective treatment option to slow down neurodegeneration and reducing associated symptoms. In this regard, different compounds that contain antioxidant properties like vitamin E, vitamin C, coenzyme Q10 and glutathione (GSH) have been examined to attenuate neurodegenerative symptoms (Sano et al., 1997). Supplementation of vitamin E early in life potentially attenuates the risk of PD (Golbe et al., n.d.). However, another study showed that vitamin E oral intake for five months did not show any effect on the increase of vitamin E levels in ventricular cerebrospinal fluid in PD patients (Pappert et al., n.d.). This explains the drawbacks of oral administration of antioxidants along with rapid antioxidant metabolism and limited entry across blood–brain barrier (Pappert et al., n.d.). To counteract this problem, some tiny antioxidant molecules, like ferrostatin-1 (Fer-1), have been produced, which show efficacy to reduce neurodegenerative symptoms (research and 2016, n.d.; Skouta et al., 2014). Furthermore, the stage of the disease, the method, the dose of antioxidant administration and the time are all key factors that should be considered while investigating the effects of antioxidant therapies in future studies (Gilgun-Sherki et al., 2001; Kim et al., n.d.). Understanding of the molecular pathogenesis of neurodegeneration is not well established till today. To determine the implications of ROS in various neurodegenerative diseases it is important to discover reliable and novel therapies.

2.1.2. Site of ROS generation

In most cells, the mitochondrion is the primary source of ROS production. Up to 2% of the total cellular mitochondrial O_2 consumption correspond to the generation of ROS including O_2^- under normal physiological condition (Cadenas et al., n.d.; Orrenius, 2007; Widlansky and Gutterman, 2011). There are multiple proposed ways that produce mitochondrial ROS, which are modulated mainly by the mitochondrial respiratory chain complexes (Cadenas et al., n.d.; Mancuso et al., n.d.; Widlansky and Gutterman, 2011). Inhibitors of mitochondrial complexes including rotenone (complex I inhibitor) (Li et al., 2003; Radad et al., 2006), antimycin A (complex III) (Woo et al., 2007), oligomycin (complex V) ("Oligomycin - an overview |

ScienceDirect Topics," n.d.) and FCCP (uncoupler of mitochondrial oxidative phosphorylation) (BRENNAN et al., 2006; Shabalina and Nedergaard, 2011) are reported to elevate cellular ROS production. Since 2000, large number of biochemical and structural biological studies provided increasing evidence that ETC individual complexes I–IV may assemble into supramolecular structures called as supercomplexes (SCs) (Schägger, 2002). Studies that analysed mitochondrial membrane proteins by blue native polyacrylamide gel electrophoresis (BN-PAGE) provided first evidence for the existence of SCs (Schagger, 2000). Refinement technology and cryo-electron microscopy (cryo-EM) based studies provided deeper insight into the structural organization of supercomplexes at near-atomic resolution (Gu et al., 2016; Letts et al., 2016; Sousa et al., 2016). It has been hypothesized that supramolecular organization of SCs could increase the catalytic activity of individual ETC complexes to transfer electrons through substrate channelling with high efficiency (Maranzana et al., 2013). SCs could also stabilize the assembly and integrity of individual ETC complexes, regulate the activity of ETC and prevent protein aggregation in the inner mitochondrial membrane (IMM). According to BN-PAGE analysis, approximately 80% of complex I, 65% of complex III and 15% of complex IV were found in supercomplexes of bovine heart mitochondria (Schagger, 2000). However, despite thorough studies, structural organization, physiological role of SCs and mechanisms of assembling remain to be elucidated (Acín-Pérez et al., 2008; Gu et al., 2016; Letts et al., 2016; Schagger, 2000). Interestingly, the capability of the ETC complexes for ROS generation may vary during disease conditions or among the organs (Turrens, 2003). For instance, complex I acts to contribute to the generation of most of O_2^- in the brain, while complex III is known as the primary source of O_2^- in the lung and heart (Turrens, 2003). In addition, ETC complex I and III are known as the main O_2^- generators within mitochondria (Zhou et al., 2016). In heathy state, production of ROS from complex I is generally one-half of those from complex III (Zhou et al., 2016), while under pathological conditions including accelerated aging and neurodegenerative diseases, complex I is the primary site of ROS production (Zorov et al., 2014).

2.1.3. SARM1 and ROS: a perspective

Although SARM1 localizes to the mitochondria, its specific role in ROS generation and its implication in neurodegeneration is not fully understood. A study

shows that during infection with La Crosse virus (LACV), SARM1 localizes to the mitochondria and induces ROS production, mitochondrial damage and ultimately neuronal death. Interestingly, this study showed that SARM1 interacts with the complex V ATP Synthase protein (Mukherjee et al., 2013). How this correlates to increased ROS generation and subsequent mitochondrial damage has not been studied yet. Another study showed that in the absence of SARM1, the mitochondrial poison CCCP depolarize mitochondria, deplete ATP levels, causes calcium influx, accumulate ROS, but axon degeneration is prevented. Survival of these neurons after the ROS accumulation indicates that SARM1 acts downstream of ROS generation (D. W. Summers et al., 2014). Moreover, hydrogen peroxide or paraquat treatment in neurons could generate ROS that kills wild type (WT) neurons, but SARM1 mutant neurons remain intact. Thus, ROS could either activate SARM1 by acting on its auto inhibitory N-terminal domain to initiate the cell destruction program by its SAM-TIR domain or interact with some ROS sensing proteins that regulate SARM1 (Daniel W Summers et al., 2014).

2.1.4. SARM1 in cell death regulation

A. Apoptosis

SARM1 plays a unique role in a novel form of cell destruction program, termed as Sarmoptosis (D. W. Summers et al., 2014). Without any upstream signal, SARM1 overexpression induced cell death in ~25% of cultured HEK cells. First 27 amino acids of SARM1 confers its mitochondrial localization in kidney cells (Panneerselvam et al., 2012). In primary T cells, SARM1 overexpression resulted in sequential activation of caspase -9, -3, and -8 and subsequent apoptosis. Overexpression of SARM1 induced an increase in ROS generation and a reduction in mitochondrial membrane potential. Overexpression of the anti-apoptotic gene bcl-xl and addition of a MAPK inhibitor could block this apoptosis partially. SARM1 knockdown in T-cells resulted in an increased survival and proliferation, supporting the role of SARM1 in its negative regulation of immunity. SARM1 overexpression in COS-1 cells resulted in JNK redistribution and mitochondrial clumping, although no cell death has been reported in this case (Panneerselvam et al., 2013). SARM1 connects mitochondria to microtubules, and also brings JNK3 to mitochondria. In neurodegenerative diseases, translocation of JNK3 to mitochondria, promotes binding and inhibiting the antiapoptotic proteins, Bcl-2 and Bcl-xL and mediating the

phosphorylation and oligomerization of the pro apoptotic protein BAD. It also mediates translocation of the pro apoptotic protein BAX from the cytoplasm to mitochondria (Kim et al., 2007). It was shown that SARM1 translocates to nucleus and stabilizes lamins and prevents DNA fragmentation during inflammation mediated apoptosis in embryonic kidney cells (Gong et al., 2016).

In the CNS, the damage associated molecular patterns (DAMPS) are produced by both pathogenic and non-pathogenic insults. Dying cells may release exosomes containing RNA and/or DNA which can stimulate endosomal TLRs. TLR7 and TLR9 are involved in this signalling pathway. It was shown that in neurons, SARM1 localizes to the mitochondria after TLR stimulation. Endosomal TLR activation induces apoptosis in neuron and SARM1 is necessary for TLR7/TLR9 mediated neuronal apoptosis. This pathway is specific to neurons because stimulation of other CNS cells like microglia and astrocytes with the same endosomal TLR ligands mediates cytokine production but not apoptosis (Mukherjee et al., 2015).

B. SARM1 and mitophagy

Recent works have suggested that PTEN-induced putative kinase 1 (PINK1) is stabilized during the loss of mitochondrial membrane potential and the accumulated PINK1 mediates translocation of Parkin (a PD-linked E3 ubiquitin ligase) from the cytoplasm to mitochondria. Parkin ubiquitinates mitochondrial outer membrane proteins, such as VDAC1 and MFN1/2 and the damaged mitochondria containing ubiquitinated proteins on their surface are the target for the autophagy via the proteasome system. PINK1 forms a complex with SARM1 and TRAF6, which helps in stabilization of PINK1 on depolarized mitochondria. It was found that PINK1 interacts with SARM1 through its N-terminal region (Murata et al., 2013). However, excessive autophagic activation might induce autophagic programmed cell death. Recent papers have shown that NAD^+ depletion induces mitophagy and autophagy. NAD^+ is a cofactor for many proteins, including SARM1, Sirtuins (SIRT1 to SIRT7), PARP (poly [ADP-ribose] polymerase) and CD38. SARM1 is a NAD^+ consuming enzyme. Increased NAD^+ may inhibit mitophagy/ autophagy through mitochondrial SIRT4, mitochondrial SIRT5, cytoplasmic SIRT2, and the DNA damage sensor PARPs. Hence activation of SARM1 may indirectly induce autophagy through NAD^+ depletion (Fang, 2019).

2.1.5. Calcium flux in neurodegeneration

Immediately after injury, axonal calcium levels rise (Adalbert et al., 2012; Knöferle et al., 2010; Ziv and Spira, 1993). Ethylene glycol tetra acetic acid (EGTA), chelator of calcium, strongly blocked axon degeneration after injury when added to the cell culture media (Schlaepfer and Bunge, 1973) and addition of calcium ions back to the media reversed this calcium blockage (George et al., 1995). Cobalt or manganese ions mediated blockage of calcium channels also strongly inhibited injury-induced axon degeneration *in vitro* (George et al., 1995). In the absence of injury, spontaneous axon degeneration was induced after the addition of calcium ionophores, suggesting that influx of calcium is necessary and sufficient to induce axon degeneration (George et al., 1995). Inhibition of voltage gated L-type calcium channels could block injury-induced axon destruction *in vitro* (George et al., 1995) and *in vivo* (Knöferle et al., 2010) whereas other types calcium channels did not show such blockage, suggesting that after transection these channels specifically allow calcium into the axon.

Within a cell, calcium flux can activate a series of intracellular processes such as protein degradation because of calcium-dependent cysteine proteases calpains. Inhibition of calpain could suppress neurodegeneration weakly in the distal side of severed axon *in vitro* (George et al., 1995; Zhai et al., 2003). In fact, fragmentation was delayed *in vivo* by genetically expressed calpain inhibitors. Calpain plays a role in the fragmentation phase of neurodegeneration specifically, as it was observed that a genetically encoded calpain inhibitor prevents neurofilament breakdown specifically but not microtubule destruction (Ma et al., 2013). But the calpain inhibitors mediated protection is much more weaker than the protection with EGTA treatment, inferring that neurodegeneration occurs through another parallel calcium-dependent mechanism (Park et al., 2013). Interestingly, axons have an intrinsic mechanism to buffer axonal calcium levels; mitochondria, where calcium levels rise to compensate this loss. However, the normal buffering capacity of mitochondria is not enough to combat the injury mediated calcium rise (Sievers et al., 2003).

However, it remains unclear whether calcium is required for the initial activation steps only or throughout the entire neurodegeneration, as it has not been reported yet whether degeneration could be stalled by removing the extracellular calcium after microtubule breakdown (latent phase). Recently, a ground-breaking

finding showed that SARM1 can catalyse the production of Cyclic ADP-ribose (cADPR) and nicotinic acid adenine dinucleotide phosphate (NAADP). These are two distinct messengers that mobilize the endoplasmic and endo-lysosomal calcium stores, respectively (Lee and Zhao, 2019). Therefore, it might be possible that SARM1 is playing as a Ca^{2+} -signalling enzyme. However, further investigation is required to determine its role in this signalling pathway.

2.1.6. Inflammatory response in neurodegenerative diseases: Does SARM1 play role?

Even though activation of immune responses and subsequent inflammation are consistently linked to aging (Chung et al., 2009), it has been not very easy to explain the role of inflammation in neurodegeneration (Ransohoff, 2016). Inflammation helps to build the protective response by which immune cells react in an efficient way against unwanted cells or debris (Karin and Clevers, 2016). For example, in the intestinal epithelium inflammation is a primary response against pathogenic microorganisms. Alterations of metabolism observed in aging cells (stress signals, loss of proteostasis, DNA damage) affect the immune response against foreign particles in the intestine and it seems the reason why elderly individuals are more susceptible to infection (Ayyaz and Jasper, 2013).

Immune responses can be generated by the nervous system, and microglia and dendritic cells command most of these processes (Fig. 32) (Carson et al., 2006). Macrophages reach sites of CNS injury where they promote both repair and injury. These cells are defined as different types including the proinflammatory, neurotoxic M1 cells, and the M2 cells, that mediate remyelination and axon growth (Kigerl et al., 2009). Morphologically, inflammation in the CNS is associated with a different shaped microglia, after an acute damage which looks hypertrophic, or after aging and neurodegeneration which looks dystrophic (Ransohoff, 2016). On the other hand, inflammatory response associated to Wallerian degeneration post injury of the nervous system. In this process, glial cells induce fragmentation of axons, isolation and conversion of myelin into lipid droplets even before macrophages reach the site (Stoll et al., 1989). Subsequently, the chemokines and cytokines levels such as IL-1 and TNF-α are upregulated, resulting in the recruitment of macrophages (Gillen et al., 1998; Liefner et al., 2000).

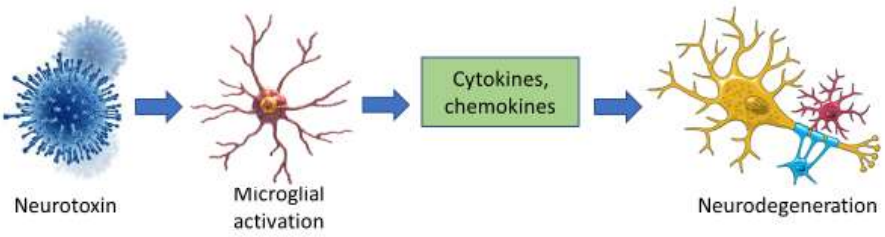

Fig. 32. Relationship between microglial activation and neuronal death. Neurotoxins may induce microglial activation that favours neuroinflammation, leading to neuronal death

Multiple sclerosis (MS) is considered as the most classic neurodegenerative disease associated with inflammation. MS is an autoimmune disease and characterized by demyelination dispersed throughout the CNS and is triggered by CD4+ T helper lymphocytes (Lucchinetti and Bruck, 2004). Mitochondria plays a major role in the mechanism of MS, affecting the healthy relation between axons and glia through numerous defects including deregulation of oxidative stress, Ca^{2+} imbalance because of excessive proinflammatory cytokines, impaired production of energy and mitochondrial autophagy (Patergnani et al., 2017).

One more interesting connection between inflammation, axonal degeneration and aging was made after the discovery of SARM1 which is required for the axon degeneration (Osterloh et al., 2012). SARM1 is a pro-degenerative molecule that mediates NAD^+ loss by its TIR domain and works after injury to trigger degeneration (Essuman et al., 2017; Gerdts et al., 2015; Summers et al., 2016). A critical aspect of the pathway is that SARM1 overexpressed cell autonomously induces axonal degeneration, a major finding considering the role of this pro-degenerative molecule in immune responses (Carty et al., 2006). Myd88, TRIF and SARM1 are Toll-like receptors (TLRs) adaptors and as they express in neurons, they are able to generate cytokines in response to different pathogen infection (Chen et al., 2011; Lin et al., 2014). Over a decade ago after analysing family-based human linkage disequilibrium studies, SARM1 was defined as a candidate gene implicated in the onset of hereditary inflammatory diseases (Mink and Csiszar, 2005). SARM1 has been reported to modulate TNF-α production in the brain to restrict viral infection (Szretter et al., 2009). Knockdown of SARM1 in mice can alter the expression of antiviral and inflammatory cytokines in the brain even in the absence of an immune challenge (Lin et al., 2014). These findings suggest a neuron-autonomous effect of SARM1 on cytokine expression.

2.1.7. Concluding remarks

Taken together, these studies suggest that multiple factors may play a role in the onset of age-associated neurodegeneration and subsequent disease progression. The pro-degenerative molecule SARM1 has been implicated in several pathways such as increased ROS production, apoptosis induction, mitophagy etc. However, whether SARM1 is a central regulator of these pathways or they function independent of each other, remains to be fully understood (Fig. 33).

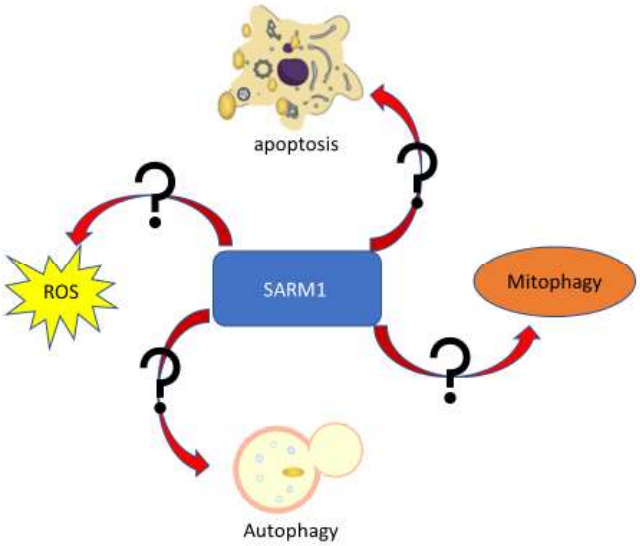

Fig. 33. SARM1 has been implicated in ROS generation, mitophagy, autophagy and apoptosis. Although, whether SARM1 is a central molecule of these pathways is yet to be explored

2.2. Materials and Methods

2.2.1. Cell culture

A. Maintenance of SH-SY5Y cells

Maintenance of SH-SY5Y cells were done as explained in previous chapter (vide Section 1.2.2.7 A).

B. Maintenance of HEK293 cells

Maintenance of SH-SY5Y cells were done as explained in previous chapter (vide Section 1.2.2.7 B).

C. Drug treatment in cell lines

Rotenone was prepared as explained in previous chapter (vide Section 1.2.2.7 C). FCCP, Oligomycin, Bafilomycin and Resveratrol (Structures shown in Fig. 34A-D) were freshly prepared as 1 mM, 1 mM, 100 mM and 10 mM stock respectively in dimethyl sulfoxide (DMSO), Antimycin (Structure shown in Fig. 34E) was prepared freshly as 5 mM stock in Ethanol and Chloroquine and NAC (Structures shown in Fig. 34F-G) were prepared freshly as 100 mM stock in water before the start of the experiment, and subsequently dilutions were made in culture medium. Neuroblastoma cells were grown in culture medium containing these substances at a dose and time dependent manner, after which they were analysed. Control cells were incubated with the same concentration of DMSO (0.2%) and Ethanol (0.2%).

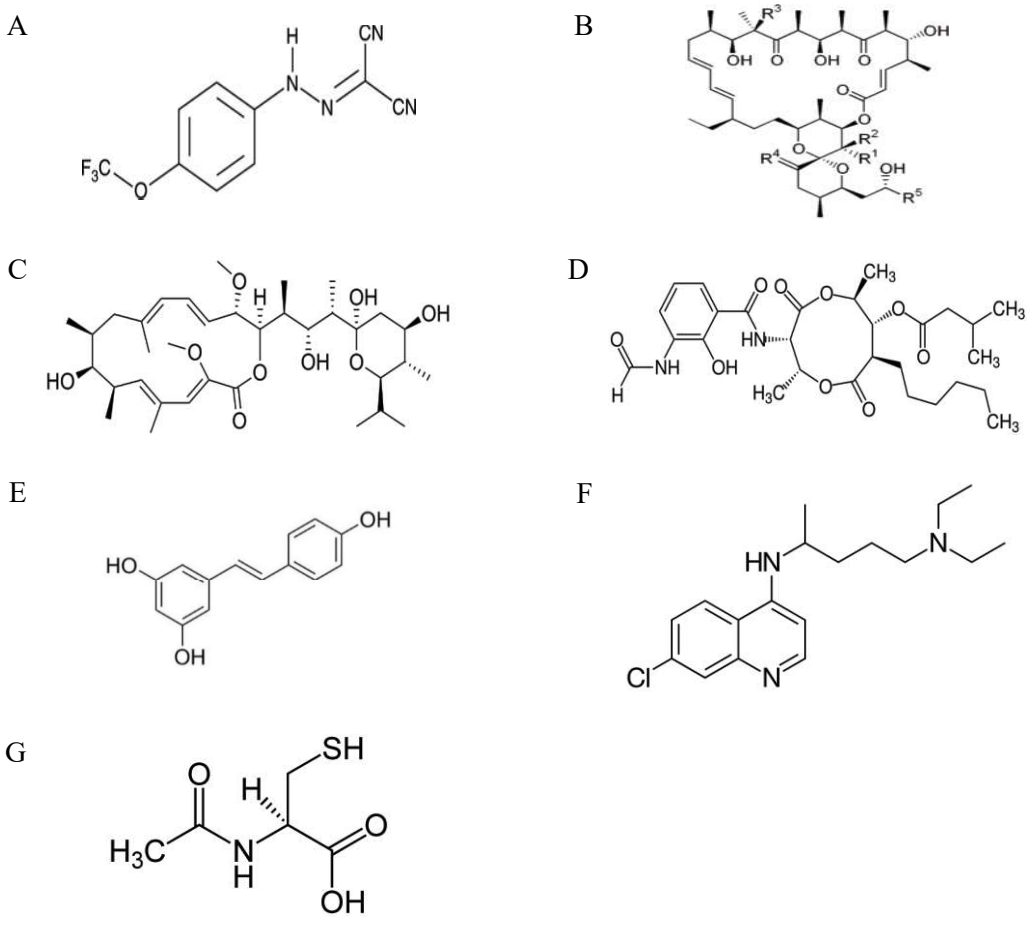

Fig. 34. Chemical structure of **(A)** FCCP, **(B)** Oligomycin, **(C)** Bafilomycin **(D)** Resveratrol **(E)** Antimycin **(F)** Chloroquine and **(G)** NAC

D. Analysis of cell growth and viability

Analysis of cell growth and viability were done as explained in previous chapter (vide Section 1.2.2.7 D).

2.2.2. Real-Time PCR

Real-Time PCR was done as explained in previous chapter (vide Section 1.2.2.8). Primer sequences used in this study are listed in Table 7. Primer 3 (v. 0.4.0) web site was chosen to design all primers (Koressaar and Remm, 2007; Untergasser et al., 2012). All sequences of nucleic acids chosen for primer designing were obtained from nucleotide database of National Center for Biotechnology Information (NCBI).

Table 7. Sequences of primers used in this study

Target genes	Sequences (size)
GAPDH (R)	5'-GCCTTCTCCATGGTGGTGAAGAC-3' (23 mer)
GAPDH (L)	5'-CCCATCACCATCTTCCAGGAGC-3' (22 mer)
GPX4 (R)	5'-CGTTGGTGACGATGCACACGAA-3' (22 mer)
GPX4 (L)	5'-AAGGACATCGACGGGCACATG-3' (21 mer)
PTGS2 (R)	5'-TCCATCCTTGAAAAGGCGCAGTTTA-3' (25 mer)
PTGS2 (L)	5'-GATGTTTGCATTCTTTGCCCAGCACTTC-3' (28 mer)
TNF α (R)	5'-GGTGTGGGTGAGGAGCAC-3' (18 mer)
TNF α (L)	5'-GAGTGACAAGCCTGTAGCCCA-3' (21 mer)
Hsp70 (R)	5'-CGTGCAGCGGTCGCTATACTC-3' (21 mer)
Hsp70 (L)	5'-GTGGGCATAGACCTGGGCTT-3' (20 mer)
SARM1 (R)	5'-GCTTGAACATGTGCTCCAAGATGCC-3' (25 mer)
SARM1 (L)	5'-GAGCAGATCCTGGTGGCTGAGAA-3' (23 mer)
IL6 (R)	5'-AGTGGCTGTCTGTGTGGGGCG-3' (21 mer)
IL6 (L)	5'-CCTTCTCCACAAGCGCCTTCGGT-3' (23 mer)
IL1β (R)	5'-CGCTTTTCCATCTTCTTCTTTGGGTA-3' (26 mer)
IL1β (L)	5'-GACAAAATACCTGTGGCCTTGGGC-3' (24 mer)
AMBRA1 (R)	5'-GCAGGAGAAGGCGGCTTG-3' (18 mer)
AMBRA1 (L)	5'-GATGTCTGGGGCGTTCTTGTATTCG-3' (25 mer)
ATG12 (R)	5'-CAGTGGGCGTGCTTTTCTCC-3' (20 mer)
ATG12 (L)	5'-GACTAGCCGGGAACACCAAGTT-3' (22 mer)
ATG16L1 (R)	5'-GGCAATCCCGGAGCTCAC-3' (18 mer)
ATG16L1 (L)	5'-CATGAGCCGGAAGACCGTCC-3' (20 mer)
ATG4A (R)	5'-CCTGGGACTTGTAGTTCTGCACTG-3' (24 mer)

Target genes	Sequences (size)
ATG4A (L)	5'-GTTTGAGAGCAGTTCCGGGCA-3' (21 mer)
ATG4B (R)	5'-GTAGCTGCGTCCATCTTCCCAG-3' (22 mer)
ATG4B (L)	5'-CGGCACACCTATTGGCCC-3' (18 mer)
ATG4C (R)	5'-CACGCAGACGTTCCGACC-3' (18 mer)
ATG4C (L)	5'-TCTTACTACGGTGGCCGGG-3' (19 mer)
ATG4D (R)	5'-ACACTGAGTTCATGGACGCGC-3' (21 mer)
ATG4D (L)	5'-TAAGATGGCGATGGCTGCGG-3' (20 mer)
ATG5 (R)	5'-CTGTCATTTTGCAATCCCATCCAGAGTTG-3' (29 mer)
ATG5 (L)	5'-CTTCTGCACTGTCCATCTAAGGATGC-3' (26 mer)
ATG9A (R)	5'-ATTCCAGAGGCTCCGCCG-3' (18 mer)
ATG9A (L)	5'-TGCTTATTGGCCAGCCTGG-3' (19 mer)
BECN1 (R)	5'-GAGCGAGGCCTCCAGAACTAC-3' (21 mer)
BECN1 (L)	5'-AGCGTCACGTCCGGTCTC-3' (18 mer)
GABARAP (R)	5'-TCTACTATCACCGGCACCCGG-3' (21 mer)
GABARAP (L)	5'-AAGAAGAGCATCCGTTCGAGAAGC-3' (24 mer)
GABARAPL1 (R)	5'-TGAGCCTGCCTGGAGGTAGA-3' (20 mer)
GABARAPL1 (L)	5'-GCTCTAGCGAAAAGCCGCC-3' (19 mer)
GABARAPL2 (R)	5'-TGGTCCTCCTTGAACATCCACTTCAT-3' (26 mer)
GABARAPL2 (L)	5'-TGCCGCCGTCGTTGTTGTT-3' (19 mer)
IRGM (R)	5'-CTCATAAAGGCAGTGTGGACCCAAA-3' (25 mer)
IRGM (L)	5'-CTGCTCAGGTCCCCTTCCAT-3' (20 mer)
MAP1LC3A (R)	5'-GTGTCTGCGGTTTGGGGG-3' (18 mer)
MAP1LC3A (L)	5'-TCACCGGGCGAGTTACCTC-3' (19 mer)
MAP1LC3B (R)	5'-CGGCATGGTGCAGGGATC-3' (18 mer)
MAP1LC3B (L)	5'-TGAGGAGATACAAGGGAAGTGGCT-3' (24 mer)
RGS19 (R)	5'-CTCAGACCCTCACCACAGCC-3' (20 mer)
RGS19 (L)	5'-CCCTCCTGCCGTCTGACTTG-3' (20 mer)
ULK1 (R)	5'-CCCTTGAAGACCACCGCG-3' (18 mer)
ULK1 (L)	5'-AGAGACCGTGGGCAAGTTCG-3' (20 mer)
DRAM1 (R)	5'-CCTTTCGCTTTTGGTTTGGACACT-3' (24 mer)
DRAM1 (L)	5'-TAGGGCCAGAGTGGGAAGG-3' (19 mer)
ATG3 (R)	5'-CTGTCTGTCCTCGCTTTGCTTCAC-3' (24 mer)
ATG3 (L)	5'-GCTACGGCAAGAGAGTGAGAAGG-3' (23 mer)
ATG7 (R)	5'-CTGCAGTTTAGAGAGTCCAGGATCCC-3' (26 mer)
ATG7 (L)	5'-CAGAGAGAGCTGTGGTTGCCG-3' (21 mer)

2.2.3. Immunoblot experiments

Immunoblot experiments were done as explained in previous chapter (section 1.2.2.9). Antibodies used in this study are listed in Table 8.

Table 8. List of primary and secondary antibodies used in this study

Protein to be detected	Primary antibody used and its dilution	Time of incubation	Secondary antibody used
β-actin	Anti- β-actin mouse monoclonal antibody (abcam) used at a dilution of 1:1000	*2h **overnight	Goat anti-mouse IgG H&L (HRP) preadsorbed (abcam) at 1/5000 dilution
ATG7	Anti- ATG7 mouse monoclonal antibody (biotechne) used at a dilution of 1:500	*2h **overnight	Goat anti-mouse IgG H&L (HRP) preadsorbed (abcam) at 1/5000 dilution
Caspase-3	Anti- Caspase-3 rabbit polyclonal antibody (abcam) used at a dilution of 1:200	*2h **overnight	Goat anti-rabbit IgG H&L (HRP) preadsorbed (abcam) at 1/5000 dilution
LC3B	Anti- LC3B rabbit polyclonal antibody (novus) used at a dilution of 1:2000	*2h **overnight	Goat anti-rabbit IgG H&L (HRP) preadsorbed (abcam) at 1/5000 dilution
Nrf1	Anti- NRF1 mouse monoclonal antibody (DSHB) used at a dilution of 1:70	*2h **overnight	Goat anti-mouse IgG H&L (HRP) preadsorbed (abcam) at 1/5000 dilution
P^{53}	Anti- p^{53} mouse monoclonal antibody (DSHB) used at a dilution of 1:40	*2h **overnight	Goat anti-mouse IgG H&L (HRP) preadsorbed (abcam) at 1/5000 dilution
P^{62}	Anti- p^{62} rabbit polyclonal antibody (novus) used at a dilution of 1:1000	*2h **overnight	Goat anti-rabbit IgG H&L (HRP) preadsorbed (abcam) at 1/5000 dilution
*Blocking with 5% skimmed milk for 30 min at room temperature. **Incubation with antibody for 2 h at room temperature or overnight at 4-degree C.			

2.2.4. Immunocytochemistry

Immunocytochemistry was done as explained in previous chapter (section 1.2.2.12).

2.2.5. ROS assay

Cellular ROS levels can be measured by a method that oxidizes 2',7' – dichlorofluorescin diacetate (DCFDA) to a fluorescence dye 2', 7' – dichlorofluorescein (DCF). The fluorescence generated from this oxidization is directly proportional to the amount of DCF ("Evaluation of Reactive Oxygen Species (ROS) Generation in Cells Using DCFDA | Biocompare.com Kit/Reagent Review," n.d.). DCF-DA is primarily reconstituted with DMSO to a stock concentration of 5 mM.

SH-SY5Y cells were cultured in 24 well plate for different time span depending on the drug treatment. To SH-SY5Y cells, 5 mM freshly prepared DCFDA was added to achieve a final concentration of 10 µM and incubated for 30 min at 37ºC. Cells were washed twice with PBS and resuspended in fresh media and fluorescence was measured at λ_{ex}=480 nm and λ_{em}=530 nm using a cell plate reader (Synergy, Bio Tek).

2.2.6. Detection of mitochondrial superoxide generation

To detect relative superoxide generation, MitoSox Red was used and manufacturer's protocol was followed. SH-SY5Y cells were cultured in 8-well chamber slides for different time span depending on the drug treatment. Cells were then treated with 5 µM Mitosox red. Then cells were incubated for 10 min at 37ºC. After the washing with PBS, the relative intensity of mitochondrial superoxide generation was analysed using a Fluorescent microscope (Leica Microsystems). Fluorescence was measured at λ_{ex}=510 nm and λ_{em}=580 nm.

2.2.7. Blocking of TNFα in SH-SY5Y cells

TNFα blocking was performed to neutralize TNF α cytotoxicity activity *in vitro*. SH-SY5Y cells were cultured in 24 well plate to obtain 70% confluency. Cells were treated with TNFα neutralizing antibody at a final concentration of 5 mg/ml for 1 h.

2.2.8 Mitochondrial and lysosomal staining

A. Mitochondrial staining: HEK293 cells were cultured in 8-well chamber slides for different time span depending on the drug treatment. To HEK293 cells, Mitotracker green was added to achieve the final concentration of 100 nM and incubated for 30

min at 37ºC. Cells were photographed under a fluorescent microscope (Leica Microsystems). Fluorescence was measured at λ_{ex}=490 nm and λ_{em}=516 nm.

B. Lysosomal staining: HEK293 cells were cultured in 8-well chamber slides for different time span depending on the drug treatment. To HEK293 cells, Lysotracker red was added to achieve the final concentration of 100 nM and incubated for 10 min at 37ºC. Cells were photographed under a fluorescent microscope (Leica Microsystems). Fluorescence was measured at λ_{ex}=577 nm and λ_{em}=590 nm.

2.3. Results

2.3.1. Studying the effect of rotenone mediated ROS generation in SARM1 induction

2.3.1.1. Rotenone treatment in SH-SY5Y cells is accompanied by increased ROS generation and antioxidant responses

Rotenone treatment results in early induction of mitochondrial ROS. A time-dependent study was carried out and it was found that rotenone induces ROS generation as early as 3 and 4 h post treatment (Fig. 35 A) prior to neurite retraction and subsequent cell death. Cells were also stained with Mitosox red and it was evident that there was an early increase in mitochondrial ROS (Fig. 35 B). However, treatment of cells with the antioxidant N-Acetyl cysteine (NAC) reduced the levels of ROS (Fig. 35C) but did not reverse rotenone induced toxicity (Fig. 35D) which indicates that ROS may not be the sole player in rotenone mediated neuronal cell death.

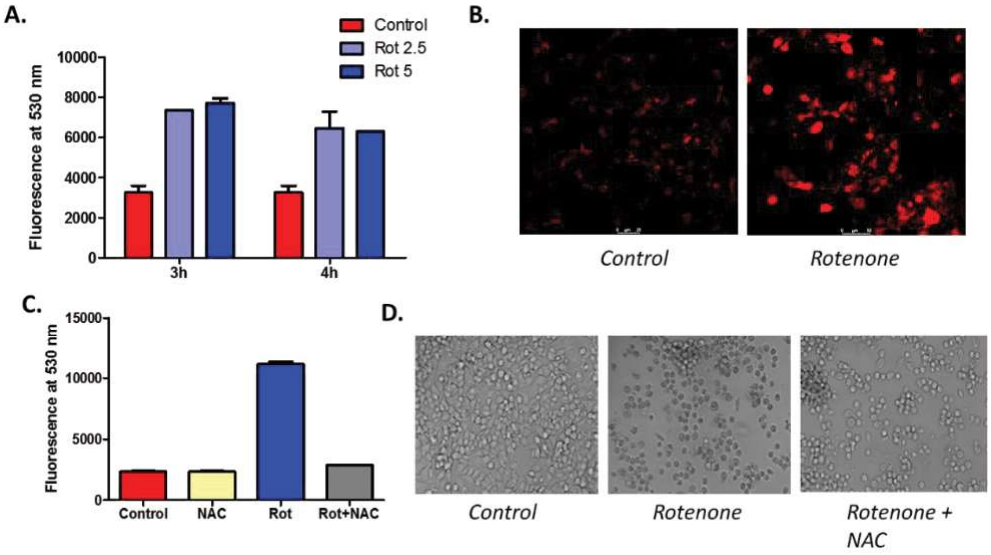

Fig. 35. SH-SY5Y cells were treated with rotenone along with NAC **(A)** ROS generation assay of SH-SY5Y cells treated with 2.5 and 5 µM of rotenone for 3 and 4 h **(B)** Mitosox

staining analysis of SH-SY5Y cells treated with 5 µM of rotenone **(C)** ROS generation assay of SH-SY5Y cells treated with 5 µM of rotenone and 5 µM of NAC **(D)** Axonal retraction of SH-SY5Y cells treated with 5 µM of rotenone and 5 µM of NAC for 24 h. Results are representative of at least three independent experiments. *p < 0.05, **p < 0.01, and ***p<0.001 compared to control sample

It has been previously reported that variety of antioxidant genes are activated by oxidative stress through cis-acting sequences on antioxidant response element (ARE) (Rodriguez-Rocha et al., 2013). In order to understand the specific role of rotenone in oxidative stress response genes, we exposed SH-SY5Y cells to 5.0 µM of rotenone for 24 h and analysed the expression of some of those genes. A significant upregulation of *Gpx4* and *Hsp70* were found in rotenone treated cells (Fig. 36A-B).

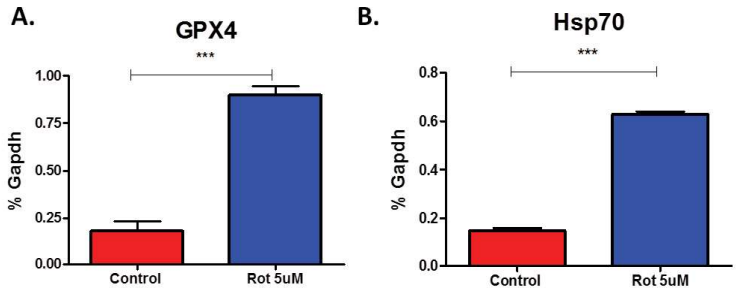

Fig. 36. SH-SY5Y cells were treated with rotenone **(A, B)** Real-time PCR analysis of SH-SY5Y cells treated with 5 µM of rotenone for 24 h. Expression of antioxidant genes from whole cell extracts were analysed

2.3.1.2. Other mitochondrial complex inhibitors also induce cell death and ROS generation in SH-SY5Y cells

To further understand the specific role of SARM1 in rotenone mediated neurotoxicity and the role of mitochondrial dysfunction, cells were exposed to other mitochondrial complex inhibitors Antimycin A, Oligomycin and FCCP (complex III and V inhibitor and uncoupler of mitochondrial oxidative phosphorylation respectively). Treatment of SH-SY5Y cells with 5.0 µM of antimycin, 10.0 µM of oligomycin and 2.0 µM of FCCP for 24 h resulted in cell death (Fig. 37A-C). Following treatment of cells with these inhibitors, there were no signs of initial axonal retraction prior to cell death (Fig. 37D-G) as observed in rotenone mediated toxicity. Instead, a significant amount of cell death was observed in these cells.

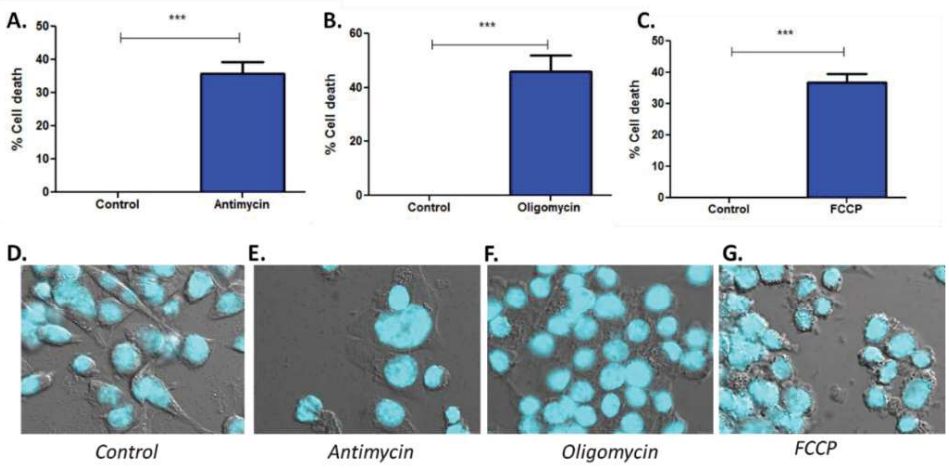

Fig. 37. MTT assay of cells treated with **(A)** antimycin (5 µM) **(B)** oligomycin (10µM) and **(C)** FCCP (2 µM) for 24 h. **(D-G)** Immunofluorescence analysis of SH-SY5Y cells treated with 5 µM of antimycin, 10 µM of oligomycin and 2 µM of FCCP for 24 h and compared to untreated control cells. DAPI staining of both the treated and untreated samples are shown. Results are representative of at least three independent experiments. *p < 0.05, **p < 0.01, and ***p<0.001 compared to control sample

A time-dependent study was carried out to correlate cell death induction with increased ROS generation and it was found that these inhibitors induced ROS generation as early as 6 h post-treatment (Fig. 38A-B).

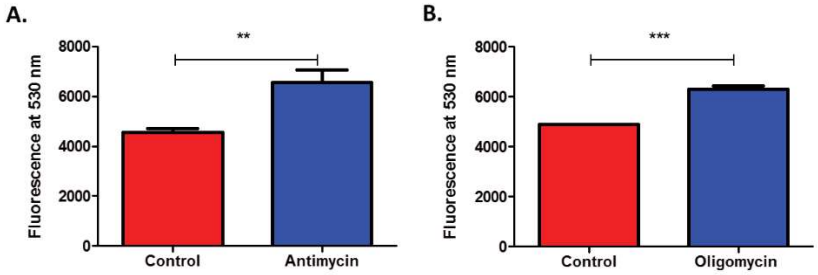

Fig. 38. ROS generation assay of cells treated with **(A)** antimycin (5 µM) and **(B)** oligomycin (10µM) for 6 h. Results are representative of at least three independent experiments. *p < 0.05, **p < 0.01, and ***p<0.001 compared to control sample

2.3.1.3. SARM1 is not induced in the presence of other mitochondrial complex inhibitors

To understand whether increased ROS production is directly correlated with SARM1 induction and deregulation of ETC complex genes, the expression of several genes of mitochondrial complex I, complex III, complex IV and complex V were analysed in SH-SY5Y cells after 24 h treatment with these inhibitors along with SARM1. Interestingly, these inhibitors did not induce the expression of *Sarm1* even at 24 h post treatment (Fig. 39).

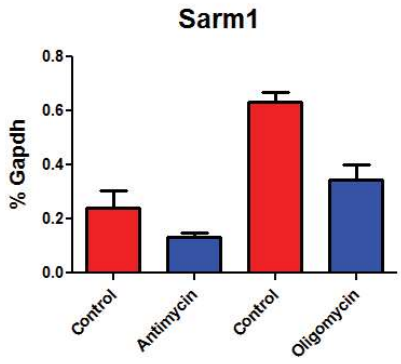

Fig. 39. Real-time PCR analysis of SH-SY5Y cells treated with antimycin (5 µM) and oligomycin (10 µM) for 24 h. Expression of *Sarm1* from whole cell extracts were analysed. Results are representative of at least three independent experiments. *p < 0.05, **p < 0.01, and ***p<0.001 compared to control sample

Further, the ETC complex genes were also differentially de-regulated as compared to rotenone treatment (Fig. 40) and we did not observe a specific upregulation of *Ndufs2* and *CoxVB*. However, Oligimycin treatment resulted in significant upregulation of the complex V gene *ATP12A*. On the other hand, *Ndufs2* expression was significantly downregulated in the presence of these inhibitors pointing towards a regulation of these genes by rotenone induced SARM1. The source of ROS within the cells plays an important role in signalling networks and this may explain why a difference in cell death pattern is observed with different mitochondrial inhibitors.

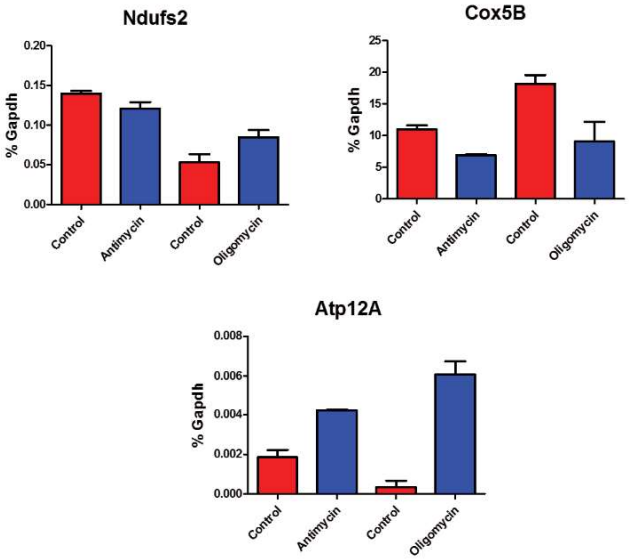

Fig. 40. Real-time PCR analysis of SH-SY5Y cells treated with antimycin and (5 µM) oligomycin (10 µM) for 24 h. Expression of ETC complex genes from whole cell extracts were analysed. Results are representative of at least three independent experiments. *p < 0.05, **p < 0.01, and ***p<0.001 compared to control sample

2.3.1.4. Overexpression of SARM1 and its mutants do not accumulate ROS in SH-SY5Y cells

It has been previously shown that SARM1 is required for mitochondrial reactive oxygen species (ROS) generation in virus-induced neuronal death (Mukherjee et al., 2013). Therefore, to understand the effect of SARM1 and its different deletion mutants on the induction of ROS generation, we overexpressed them in SH-SY5Y cells by transient transfection and checked the ROS level. We did not find any significant amount of ROS level in SARM1 overexpressed cells (Fig. 41).

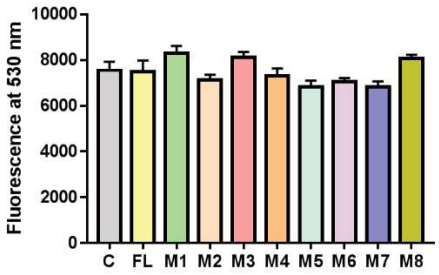

Fig. 41. ROS generation assay of cells transfected with different deletion mutants of SARM1. Results are representative of at least three independent experiments. *p < 0.05, **p < 0.01, and ***p<0.001 compared to control sample

Similar observations were also found when transfected cells were stained with Mitosox red (Fig. 42). Our results suggest that SARM1 over expression may not be directly related to ROS induction in these cells.

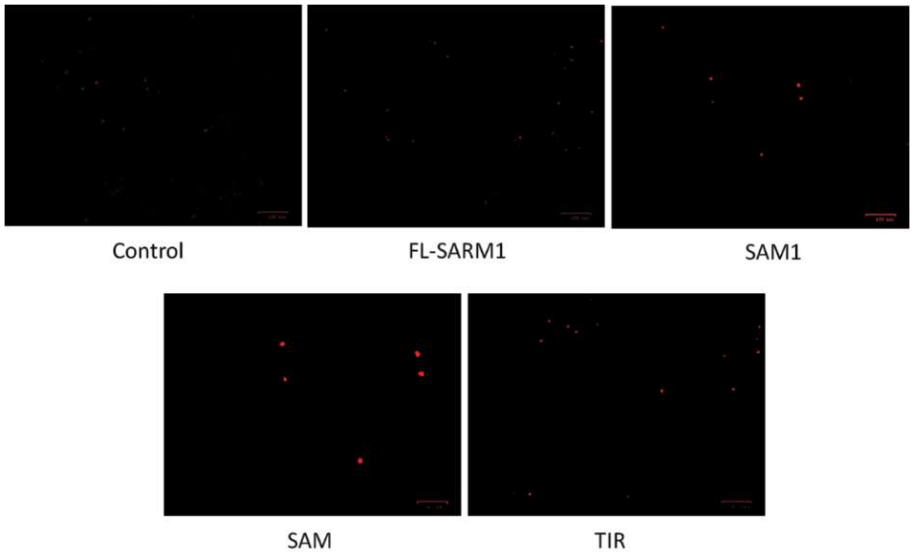

Fig. 42. Mitosox staining analysis of SH-SY5Y cells transfected with different deletion mutants of SARM1. Scale bars = 25 µm

Taken together, our results indicate that rotenone mediated ROS generation and SARM1 induction work independently of each other. Further, SARM1 played a key role in rotenone induced cell death and reduction of ROS levels did not reverse rotenone induced toxicity. Hence it was not rational to understand the site of ROS generation. Instead the remaining part of this chapter focuses on understanding what may induce SARM1 within the cells and how SARM regulate mitochondrial homeostasis by mitophagy, etc.

2.3.2. Regulation of rotenone induced autophagic pathway and its effect on SARM1

2.3.2.1. Rotenone inhibits autophagic flux that may result in SARM1 induction in SH-SY5Y cells

Since treatment of cell with the antioxidant NAC did not reverse cell death nor SARM1 induction, we hypothesized there could be other forms of stress within the cells that may lead to the upregulation of SARM1 and subsequent cell death. In neurodegenerative diseases such as Parkinson's disease (PD), autophagy has been implicated to play a protective role. However, excessive autophagic activation mediates autophagic programmed cell death. ROS over-generation, reduction of mitochondrial membrane potential or apoptosis rate elevation occurs in rotenone treated human neuroblastoma cell line SH-SY5Y. The number of autophagic vacuoles were increased in rotenone based PD models *in vitro* and *in vivo (Xiong et al., 2013).* Few reports have suggested that NAD-dependent Sirt1 regulates autophagy and NAD^+ depletion results in impaired autophagic response (Lee et al., 2008). Again, previously it was also shown that mitochondrial ETC complex I inhibitors induce autophagic cell death via reactive oxygen species generation (Chen et al., 2007). Since rotenone treatment and increased SARM1 was associated with reduction in NAD^+ levels, we tried to determine the status of autophagy machinery in rotenone treated cells. We analysed several autophagy related genes (early and late) at 3 h, 6 h and 24 h post treatment and found an initial increase in *Atg* genes associated with early autophagy induction (Fig. 43). However, the expression of genes involved in autophagosome-lysosome fusion was downregulated at all the time points indicating that autophagy might be induced but not completed following rotenone treatment.

Fig. 43. Heat map presentation of the Q-PCR analysis of SH-SY5Y cells treated with rotenone (5 µM). Autophagy related genes were analysed following 3 h, 6 h and 24 h post treatment. Results are representative of at least three independent experiments. *p < 0.05, **p < 0.01, and ***p<0.001 compared to control sample

Analysis of the key autophagy proteins showed increased levels of the early autophagy protein ATG7 (Fig. 44A). Increased levels of LC3B which indicates autophagy induction was also observed in these cells (Fig. 44A-B). However, there was increased accumulation of p62 protein in these cells (Fig. 44A) indicating that there was defective autophagic flux which could be correlated with increased energy deficits within the cell. p62 accumulation was also observed following immunofluorescence analysis (Fig. 44C).

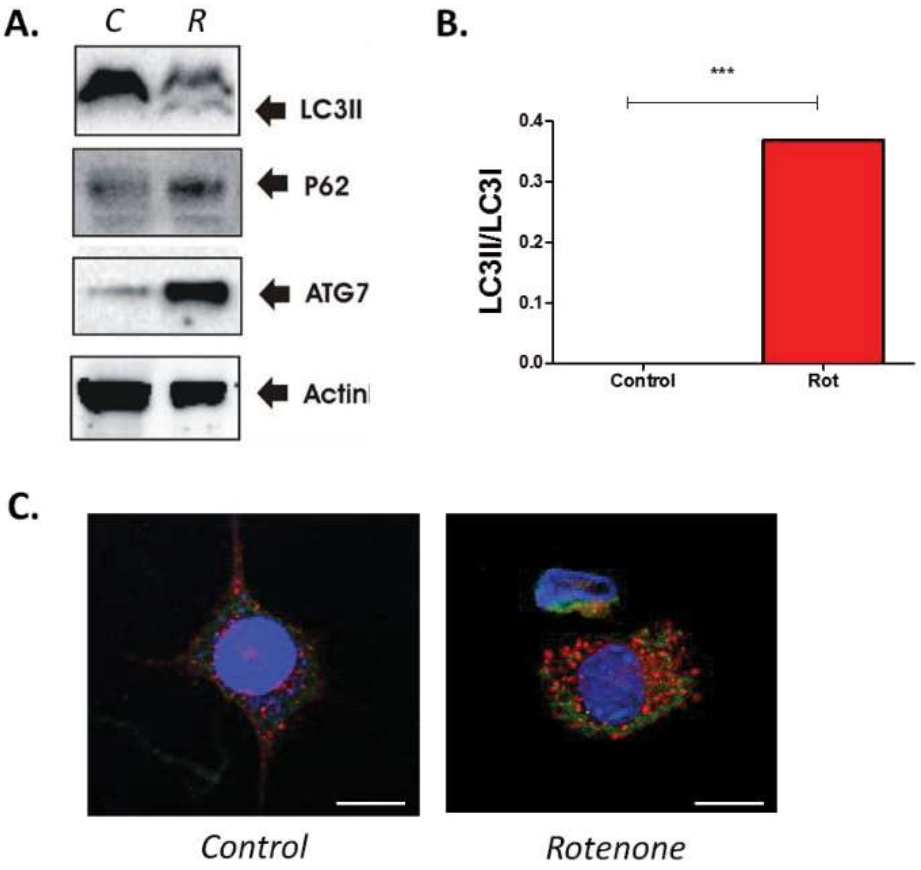

Fig. 44. SH-SY5Y cells were treated with rotenone **(A)** Analysis of p62, ATG7 and LC3B protein levels in the whole cell extracts of cells treated with rotenone (5 µM) at 24 h. β-actin was used as a loading control. **(B)** Quantification of LC3II/LC3I was done to determine the LC3B concentration in control vs treated cells **(C)** Immunofluorescence analysis of SH-SY5Y cells treated with 5 µM of rotenone for 24 h and compared to untreated control cells. DAPI (blue) tubulin (green) and p62 (red) staining of both the treated and untreated samples are shown. Scale bars = 10 µm

Excess autophagy has been known to induce cellular death termed 'autosis'. Further, inhibition of autophagic flux may accumulate stress within the cells and skew the balance towards increased cell death. Treatment with the autophagy inhibitor chloroquine (100 µm) which is a lysosomal inhibitor, significantly increased rotenone (5 µM) mediated cell death (Fig. 45A) along with several fold increase in *Sarm1* expression (Fig. 45B).

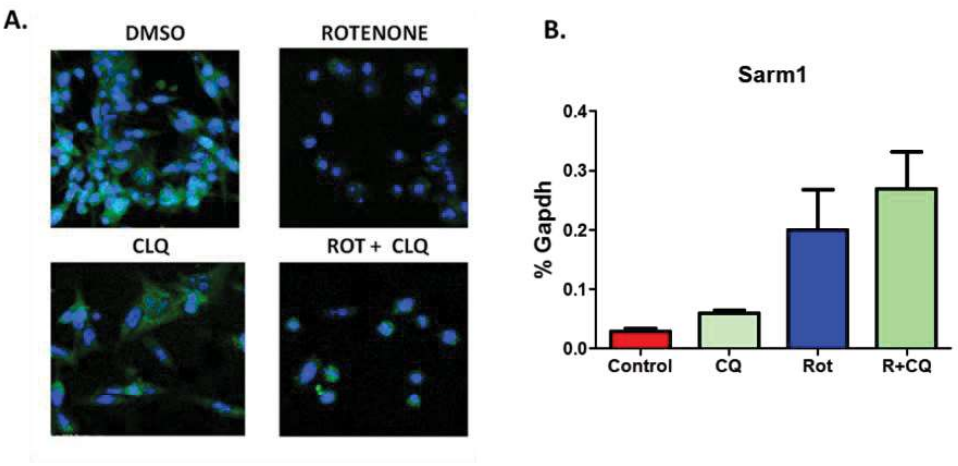

Fig. 45. SH-SY5Y cells were treated with rotenone along with chloroquine **(A)** Immunofluorescence analysis of SH-SY5Y cells treated with 5 µM of rotenone and chloroquine (100 µM) for 24 h and compared to untreated control cells. DAPI (blue) and MAP2 (green) staining of both the treated and untreated samples are shown. Scale bars = 25 µm **(B)** Real-time PCR analysis of SH-SY5Y cells treated with rotenone (5 µM) and chloroquine (100 µM) for 24 h. Expression of *Sarm1* from whole cell extracts were analysed. Results are representative of at least three independent experiments. *p < 0.05, **p < 0.01, and ***p<0.001 compared to control sample

SARM1 has been shown to mediate a distinct form of apoptosis termed 'Sarmoptosis'. Our results in rotenone treated cells suggest induction of apoptosis at 24 h post-treatment (Fig. 46) and not at 6 h (data not shown). Since axonal retraction occurred prior to SARM1 induction we explored pathways that may lead to SARM1 induction and cellular apoptosis. Our results indicate that rotenone may play an important role to inhibit autophagic flux which results in SARM1 induction that further induces apoptosis in the later stage of rotenone toxicity.

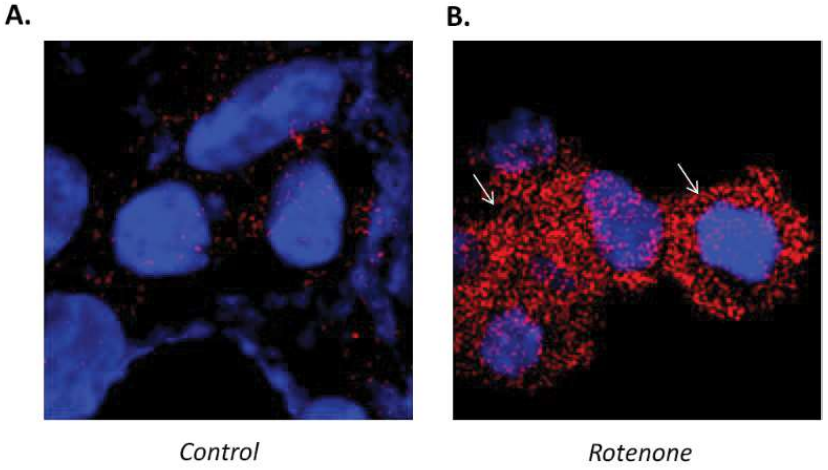

Fig. 46. SH-SY5Y cells were treated with rotenone. **(A, B)** Immunofluorescence analysis of SH-SY5Y cells treated with 5 µM of rotenone **(B)** for 24 h and compared to untreated control

cells **(A)**. DAPI (blue) and caspase-3 (red) staining of both the treated and untreated samples are shown. Scale bars = 5 µm

2.3.2.2. NR partially reverses rotenone induced de-regulation of autophagy genes in SH-SY5Y cells

In our previous experiments, it has been found that NR treatment reduced rotenone mediated cell death and SARM1 upregulation in SH-SY5Y cells. Therefore, to determine whether NR could also reverse the rotenone mediated inhibition of autophagic flux, we treated our cells with 0.5 mM of NR along with 5 µM of rotenone and analysed several autophagy related genes at 24 h post treatment. Interestingly, the genes were restored to normal levels following NR treatment (Fig. 47), suggesting that NR mediated reversal of cellular stress that was induced by rotenone was sufficient to restore the cellular homeostasis in SH-SY5Y cells.

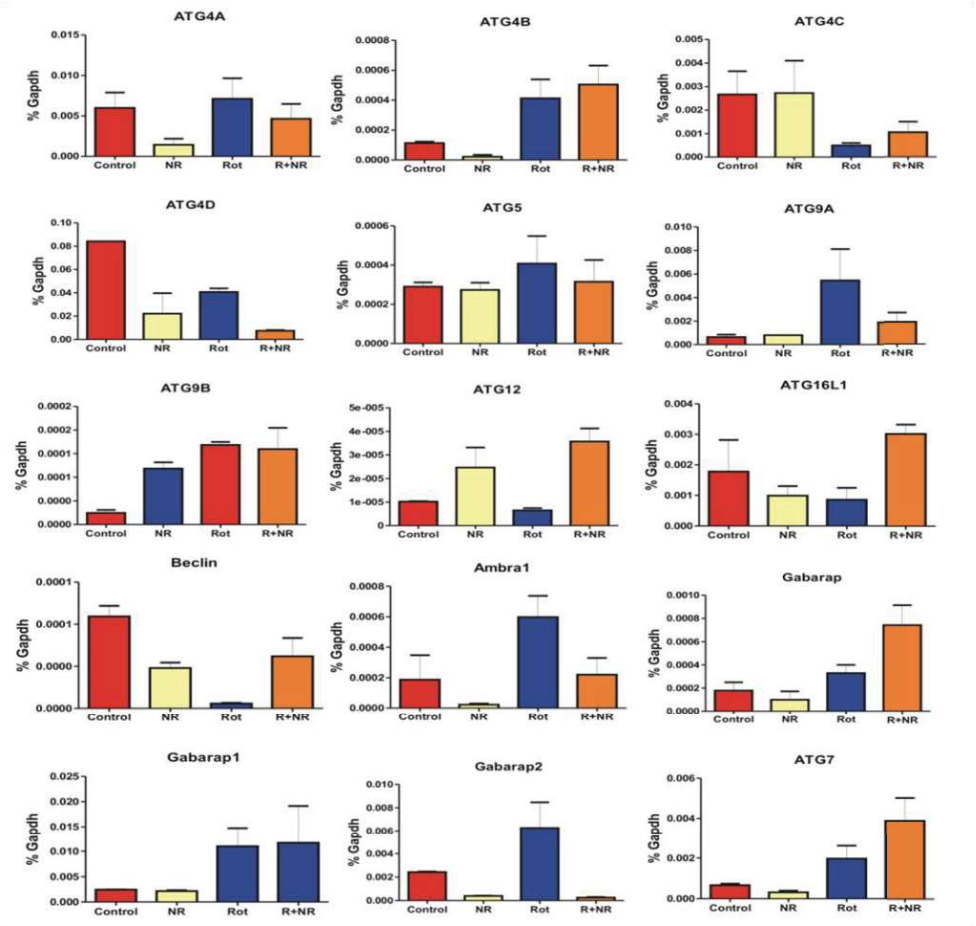

Fig. 47. Real-time PCR analysis of SH-SY5Y cells treated with rotenone (5 µM) and NR (0.5 mM). Autophagy related genes were analysed following 24 h post treatment. Results are representative of at least three independent experiments. *p < 0.05, **p < 0.01, and ***p<0.001 compared to control sample

2.3.2.3. The autophagy inhibitor bafilomycin reversed rotenone induced cell death and prevents SARM1 induction in SH-SY5Y cells

Our previous observation suggests that inhibiting autophagy with the lysosomal inhibitor chloroquine significantly increases rotenone mediated cell death and *Sarm1* expression. Surprisingly, treatment with another autophagy inhibitor bafilomycin had opposing effects on the cells. Bafilomycin is an inhibitor of vacuolar H^+-ATPase (V-ATPase) and prevents lysosomal acidification. Pre-treatment of SH-SY5Y cells with bafilomycin (100 nM) reversed rotenone mediated neurite retraction as evident by MAP2 staining (Fig. 48A) and concomitant reduction in *Sarm1* expression (Fig. 48B). This is very intriguing as most studies have used chloroquine and bafilomycin interchangeably as they inhibit a similar step in autophagy. Further, in-depth analysis is required to understand the molecular mechanism behind this significant reversal of cell death induced by bafilomycin following rotenone treatment.

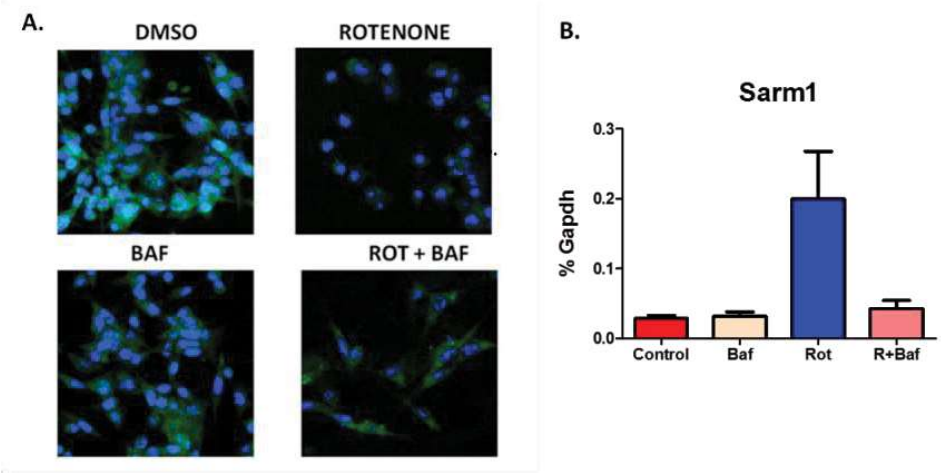

Fig. 48. SH-SY5Y cells were treated with rotenone along with bafilomycin **(A)** Immunofluorescence analysis of SH-SY5Y cells treated with 5 µM of rotenone and bafilomycin (100 nM) for 24 h and compared to untreated control cells. DAPI (blue) and MAP2 (green) staining of both the treated and untreated samples are shown. Scale bars = 25 µm **(B)** Real-time PCR analysis of SH-SY5Y cells treated with rotenone (5 µM) and bafilomycin (100 nM) for 24 h. Expression of *Sarm1* from whole cell extracts were analysed. Results are representative of at least three independent experiments. *p < 0.05, **p < 0.01, and ***p<0.001 compared to control sample

2.3.2.4. Rotenone treatment blocked mitophagy in HEK293 cells.

As previously described HEK293 cells are good model system to study SARM1 mediated pathway regulation as they are one of the few cells that express endogenous level of *Sarm1*. Since there was excess accumulation of mitochondrial

ROS and increased mitochondrial damage in rotenone treated cells, we checked the status of mitophagy, a process of clearance of damaged mitochondria via the autophagy process. However, no standard protocol is available to monitor mitophagy within the cells. Following rotenone treatment (500 nM) for 24 h, cells were simultaneously stained with Mitotracker green and Lysotracker red dyes and were monitored on a confocal microscope for co-localization analysis. Rotenone treatment showed mitochondrial swelling and there was partial co-localization of the signals (Fig. 49) indicating that mitophagy is probably induced in rotenone treated cells but not completed as previously described.

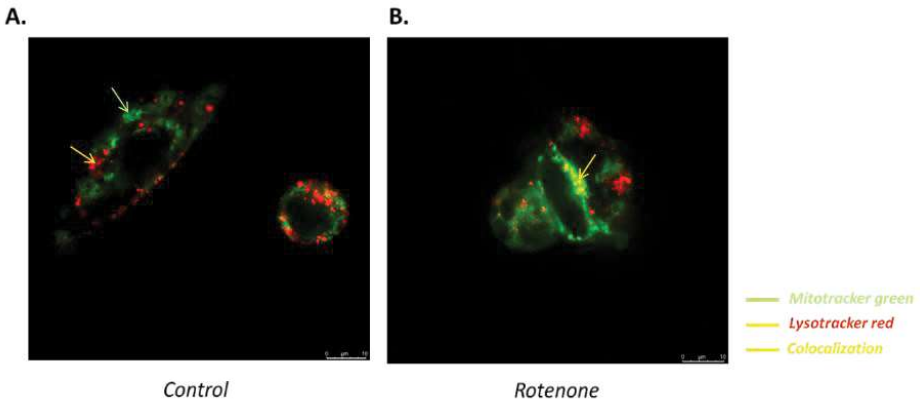

Fig. 49. HEK293 cells were treated with rotenone. **(A, B)** Immunofluorescence analysis of HEK293 cells treated with 500 nM of rotenone **(B)** for 24 h and compared to untreated control cells **(A)**. Mitotracker green and Lysotracker red staining of both the treated and untreated samples are shown. Scale bars = 10 µm

2.3.3. Inflammatory responses within the neuronal cells might trigger SARM1 activation SH-SY5Y cells

Previously it has been shown that SARM1 modulates TNF-α production to restrict viral infection in the brainstem (Lin et al., 2014; Pan and An, 2018). Taking cue from this, we tried to understand the inflammatory responses in rotenone treated cells, as rotenone treatment is directly related to SARM1 upregulation as shown in our previous result. However, we found that rotenone induced *TNF-α* expression as early as 6 h post treatment, which remained similar at 24 h post-treatment (Fig. 50A). However, there was no significant induction of the other inflammatory genes IL1b and IL^ at these time points (Fig. 50B-C).

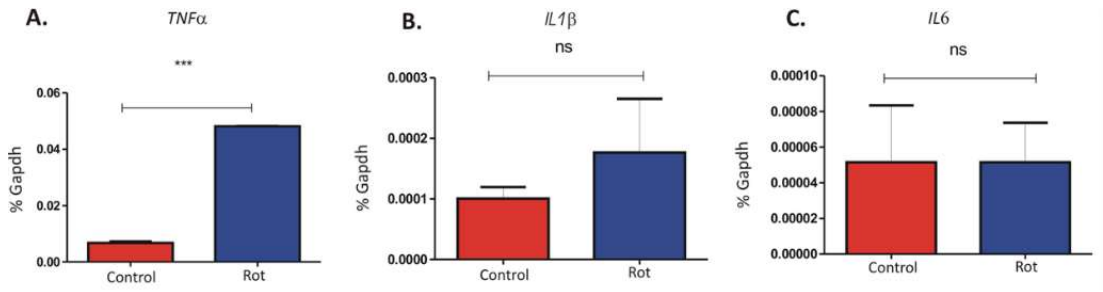

Fig. 50. SH-SY5Y cells were treated with rotenone. **(A-C)** Real-time PCR analysis of cells as treated with rotenone (5 µM). *TNFα* **(A)**, *IL1β* **(B)** and *IL6* **(C)** genes was analysed following 24 h post-treatment

When these cells were treated with varying doses of resveratrol (5 and 20 µM), they showed a significant reversal of the inflammatory response (Fig. 51A). Interestingly, in these cells, *TNF-α* expression preceded SARM1 induction at 6 h post-treatment (Fig. 51B), indicating that inflammatory responses might trigger SARM1 activation in these cells. However, blocking TNF-α by using neutralizing antibody against it, following rotenone treatment for 24 h and reduced TNF-α mRNA levels but there was a moderate upregulation of *Sarm1* in these cells (Fig. 51C-D). Further, TNF-α blocking did not result in reduction of rotenone mediated cell death (Fig. 51E), suggesting that moderate increase in *Sarm1* expression was sufficient to promote rotenone induced cell death.

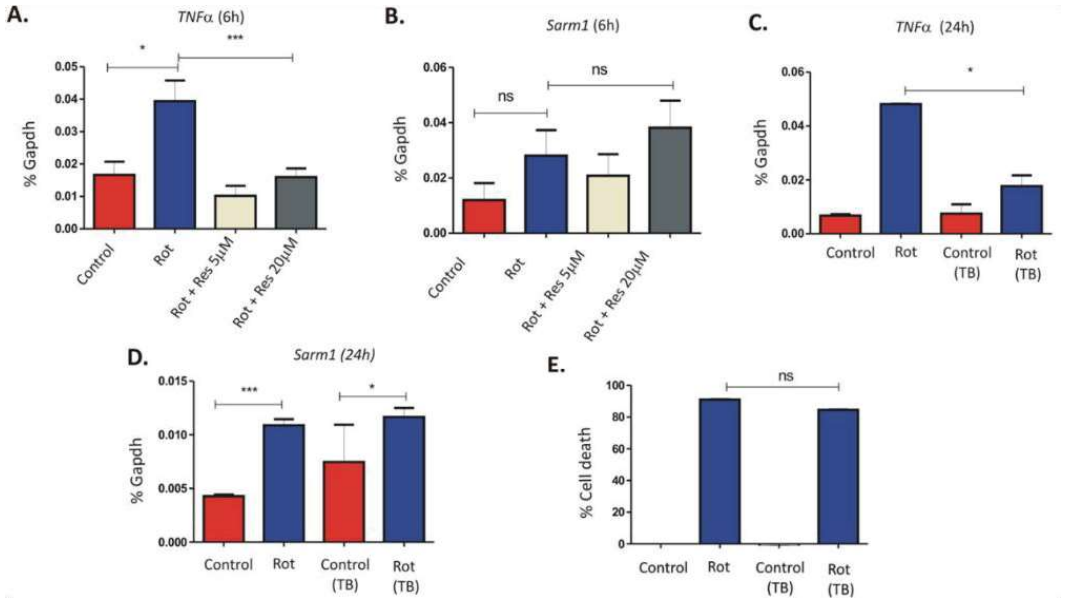

Fig. 51. SH-SY5Y cells were treated with rotenone along with resveratrol **(A, B)** Real-time PCR analysis of cells as treated with rotenone (5 µM) in the presence or absence of resveratrol (5 or 20 µM as indicated). *TNFα* **(A)** and *Sarm1* **(B)** genes were analysed following 6 h post-treatment. **(C-E)** SH-SY5Y cells were treated with rotenone along with

TNFα blocker. Real-time PCR analysis of cells treated with rotenone (5 μM) in the presence or absence of neutralizing antibody against TNFα (5 mg/ml). The expression of both *TNFα* **(C)** and *Sarm1* **(D)** were analysed following 24 h post-treatment. **(E)** MTT assay of cells treated with rotenone (5 μM) in the presence or absence of neutralizing antibody against TNFα (5 mg/ml) for 24 h. Results are representative of at least three independent experiments. *p < 0.05, **p < 0.01, and ***p<0.001 compared to control sample

2.4. Discussion

In our previous study we have observed that rotenone treatment to SH-SY5Y cells serves as an excellent model to study the function of endogenous SARM1. Rotenone not only induced markedly higher expression of *Sarm1*, we show here for the first time that *Sarm1* is required for rotenone induced toxicity in SH-SY5Y cells. Since our results indicated that SARM1 induction correlated with the increased expression of some of the ETC genes, we sought to determine whether this could play a role in the increased ROS generation following rotenone treatment. Our results indicate that rotenone treatment results in increased ROS generation and antioxidant responses. Treatment of cells with other mitochondrial complex inhibitors like Antimycin (Complex III inhibitor), Oligomycin (Complex V inhibitor) and FCCP (uncoupler of mitochondrial oxidative phosphorylation) also induced early ROS generation and cell death, but unlike rotenone, these treatments did not upregulate *Sarm1* expression and differentially deregulated expression of ETC complex gene. In fact, in the presence of these inhibitors, *Ndufs2* expression was significantly downregulated unlike rotenone suggesting a regulatory role of SARM1 on the expression of these genes. The difference in cell death pattern that is observed in different mitochondrial inhibitors might be a result of different source of ROS within the cells. Interestingly, over-expression of *Sarm1* and its deletion mutants failed to accumulate ROS in these cells. Further, contrary to our hypothesis we found that pre-treatment with the antioxidant NAC reduced rotenone induced ROS levels but did not reverse *Sarm1* expression or accompanying cell death. Taken together, these results indicate that rotenone induced ROS generation and induction of SARM1 work independently of each other where SARM1 acts as the final trigger of cell death following rotenone treatment. Since our study focused on elucidating the mechanism of SARM1 in the regulation of mitochondrial homeostasis, we proceeded to study other signalling network that may regulate this process.

Removal of damaged mitochondria by the process of autophagy (mitophagy) is an important cellular mechanism for maintaining mitochondrial homeostasis and preventing ROS accumulation in the cells. Accumulation of damaged mitochondria may trigger increased ROS production which in a vicious cycle may damage the neighbouring mitochondria. Few reports have suggested that autophagy is regulated by NAD^+ dependent Sirt1 and NAD^+ depletion leads to impaired autophagic response (Lee et al., 2008). Again, previously it was also shown that mitochondrial ETC complex I inhibitors induce autophagic cell death via reactive oxygen species generation (Chen et al., 2007). Since rotenone treatment and increased SARM1 was associated with reduction in NAD^+ levels, we tried to determine the status of autophagy machinery in rotenone treated cells. We observed increased expression of several early autophagy related genes (*Atg*) as early as 3 h following rotenone treatment. Interestingly, the expression of genes involved in autophagosome-lysosome fusion was downregulated at all the time points (early and late) suggesting that autophagy might be induced but not completed post rotenone treatment. This was confirmed by LC3 cleavage into LC3B and increased accumulation of p62 within the cells indicating a defective autophagy flux. We also checked the status of mitophagy by simultaneously staining the cells with Mitotracker green and Lysotracker red dyes. Their co-localization analysis on a confocal microscope did show a few yellow dots indicating mitophagy, however most of the mictochondria did not co-localize with the lysosome.

Pre-treatment with both the calcium channel blocker Nimodipine and the NAD^+ supplement NR could partially reverse de-regulation of autophagy genes, suggesting that reduction of cellular stress might restore cellular homeostasis. Further inhibition of autophagy by the autophagy inhibitor chloroquine resulted in significant cell death that was accompanied by much higher *Sarm1* expression. Taken together these results suggest that accumulating stress following rotenone treatment might trigger SARM1 within the cell that further induce cellular apoptosis as evident by the increased levels of active caspase-3.

Interestingly, treatment with another autophagy inhibitor bafilomycin had remarkable protective effect on rotenone mediated cell death accompanied by reduced SARM1 levels. It may be speculated that SARM1 might interact with the H^+-ATPase and block the function of bafilomycin. To further explore the pathways involved,

RNA sequencing analysis are underway to determine the effect of bafilomycin in rotenone treated cells.

To further understand the implication of rotenone mediated SARM1 in inflammatory responses, another important mediator of cellular homeostasis, we determined expression of *TNF-α* and interestingly, in these cells, *TNF-α* expression preceded SARM1 induction. However, there was no induction of other inflammatory genes *IL1β* and *IL6* in these cells. Pre-treatment of these cells with the anti-inflammatory compound resveratrol induced significant reversal of the inflammatory responses and also delayed rotenone induced cell death significantly. However, blocking TNF-α by using neutralizing antibody in rotenone treated cells, did not reduce cell death and there was a moderate upregulation of *Sarm1* in these cells. These observations indicate that moderate increase in *Sarm1* expression was sufficient to drive rotenone induced cell death. Together our findings show that blockage of autophagic flux and increased accumulation of damaged mitochondria may increase cellular stress, loss of NAD^+ and subsequently induce SARM1 which further reduces NAD^+ levels ultimately leading to apoptosis. Defective clearance of damaged mitochondria by impaired mitophagy and the regulation of inflammation-autophagy axis by SARM1 offer an exciting area that needs to be explored further.